HHS Public Access

Author manuscript

Invest Radiol. Author manuscript; available in PMC 2021 April 01.

Published in final edited form as:

Invest Radiol. 2020 April ; 55(4): 209–216. doi:10.1097/RLI.0000000000000631.

Molecular MR imaging of fibrin deposition in the liver as an indicator of tissue injury and inflammation

Iliyana Atanasova[1], **Mozhdeh Sojoodi**[2], **Helena S. Leitão**[3], **Sergei Shuvaev**[1], **Carlos F. G. C. Geraldes**[4], **Ricard Masia**[5], **Alexander S. Guimaraes**[1], **Kenneth K. Tanabe**[2], **Bryan C. Fuchs**[2], **Peter Caravan**[1,6]

[1]Athinoula A. Martinos Center for Biomedical Imaging, Massachusetts General Hospital and Harvard Medical School, Boston, MA 02129 USA.

[2]Division of Surgical Oncology, Massachusetts General Hospital Cancer Center and Harvard Medical School, Boston, MA 02114 USA.

[3]Department of Biomedical Sciences and Medicine and University Hospital Center, University of Algarve, 8005-139 Faro, Portugal.

[4]Department of Life Sciences and Coimbra Chemistry Center, Faculty of Science and Technology, University of Coimbra, 3000-393 Coimbra, Portugal.

[5]Department of Pathology, Massachusetts General Hospital and Harvard Medical School, Boston, MA 02114 USA.

[6]The Institute for Innovation in Imaging (i[3]), Department of Radiology, Massachusetts General Hospital, Boston, MA 02129 USA.

Abstract

Rationale and objectives: Liver inflammation is associated with nonalcoholic steatohepatitis and other pathologies, but noninvasive methods to assess liver inflammation are limited. Inflammation causes endothelial disruption and leakage of plasma proteins into the interstitial space and can result in extravascular coagulation with fibrin deposition. Here we assess the feasibility of using the established fibrin-specific MR probe EP-2104R for the noninvasive imaging of fibrin as a marker of liver inflammation.

Methods: Weekly 100 mg/kg diethylnitrosamine (DEN) dosing was used to generate liver fibrosis in male rats; control animals received vehicle. MR imaging at 1.5 T with EP-2104R, a matched non-fibrin binding control linear peptide (CLP), or the collagen-specifc probe EP-3533 was performed at 1 day or 7 days following the last DEN administration. Imaging data were compared to quantitative histological measures of fibrosis and inflammation.

Results: After 4 or 5 DEN administrations the liver becomes moderately fibrotic and fibrosis is the same if the animal is sacrificed 1 day (Ishak score: 3.62 ± 0.31) or 7 days (Ishak 3.82 ± 0.25) following the last DEN dose, but inflammation is significantly higher at 1 day compared to 7 days after the last DEN dose (histological activity index from 0 – 4: 3.54 ± 0.14 vs 1.61 ± 0.16,

Correspondence: Peter Caravan, PhD (caravan@nmr.mgh.harvard.edu), A. A. Martinos Center for Biomedical Imaging, 149 Thirteenth Street, Suite 2301, Charlestown MA 02129, Phone: +1 617-643-0193 Fax: +1-617-726-7422.

respectively, P<0.0001). Peak EP-2104R signal enhancement was significantly higher in animals imaged at 1 day post DEN compared to 7 days post DEN or control rats (29.0 ± 3.2% vs 22.4 ± 2.0% vs 17.0 ± 0.2%, respectively P=0.017). Signal enhancement with EP-2104R was significantly higher than CLP at 1 day post DEN but not at 7 days post DEN indicating specific fibrin binding during the inflammatory phase. Collagen molecular MR with EP-3533 showed equivalent T1 change when imaging rats 1 day or 7 days post DEN, consistent with equivalent fibrosis.

Conclusion: EP-2104R can specifically detect fibrin associated with inflammation in a rat model of liver inflammation and fibrosis.

Keywords

liver; inflammation; fibrosis; molecular imaging; EP-2104R; fibrin

Introduction

Chronic liver disease is a major cause of morbidity and mortality worldwide, and unlike other major causes of mortality, rates of chronic liver disease are increasing rather than declining (1). Currently, biopsy is used to assess disease but it is an imperfect gold standard that suffers from both intra/inter-observer variability and sampling error, and is associated with several complications. Importantly, repeated biopsies to evaluate disease progression or response to treatment are impractical due to the increased risk of complications and poor patient compliance. Nonalcoholic steatohepatitis (NASH) is a major form of chronic liver disease in the Western world, with an estimated prevalence of 5% in the general population (2). Closely associated with obesity, diabetes, and the metabolic syndrome (3), NASH is recognized as a major cause of liver-related morbidity and mortality. NASH is associated with steatosis, inflammation, and fibrosis of the liver. The emergence of NASH as an epidemic has further heightened the need for non-invasive methods that can quantitatively report on the status of the liver with respect to steatosis, inflammation, and fibrosis.

Steatosis can be accurately assessed by proton density fat fraction MRI (4, 5). Fibrosis is more challenging, for example, panels of serum biomarkers have shown some utility in the identification of fibrosis, but cannot differentiate stages of fibrosis reliably or determine rate of fibrosis progression or regression (6, 7). Ultrasound and MR elastography are effective in distinguishing advanced fibrosis (8, 9). Molecular imaging approaches have shown promise in preclinical models to stage liver fibrosis in different models, including targeting type I collagen (10–13). However methods to assess inflammation are lacking. A gadolinium-based contrast agent that is oxidized by the enzyme myeloperoxidase, causing it to be covalently bound to matrix proteins was recently reported to be able to distinguish NASH from fatty liver in mouse models (14). Limitations of this work include the need for delayed imaging and concerns regarding the retention of Gd at the locus of inflammation.

Here, we sought to determine whether molecular imaging of extravascular fibrin could be a useful way to assess hepatic inflammation. In addition to its primary function of maintaining homeostasis, coagulation is also known to play a role in downstream inflammatory and fibroproliferative processes of tissue repair (15–17). Abnormal extravascular, parenchymal

accumulation of fibrin has been previously detected in rodent models of hepatic fibrosis (18–20). Extravascular fibrin deposition is anticipated after acute injury due to vascular leakage caused by endothelial damage and the inflammatory response.

We hypothesized that in vivo quantification of parenchymal fibrin could serve as a marker of liver inflammation. The molecular magnetic resonance (MR) probe EP-2104R is a gadolinium (Gd)-based contrast agent that specifically targets fibrin with > 1000-fold higher affinity for fibrin compared to fibrinogen (21). The probe has been shown to be a sensitive method for detecting intravascular thrombi with MR imaging (MRI) in both animal models and human studies (22, 23), and has also been used to detect and quantify extravascular fibrin associated with cancer and pulmonary fibrosis (24–26). The objective this study is to investigate whether EP-2104R enhanced MRI could be used to detect inflammation in the context of liver fibrosis using an in vivo rat model.

Materials and Methods

Animal model

A total of 40 rats were used in this study. Male Wistar rats (initial weight 190 – 220 g) were given weekly intraperitoneal injections of 100 mg/kg diethylnitrosamine (DEN) formulated in phosphate buffered saline (PBS) for 4 weeks (n=22) or 5 weeks (n=7) to induce fibrosis. Subsequently, rats were divided into two sub-groups to study extravascular fibrin accumulation during an inflammatory phase 1 day after the last DEN administration (n=18) or during fibrosis in the absence of inflammation at 7 days after the last DEN administration (n=11). Control animals (n=5) received PBS for 4 weeks and were imaged one week after the 4th PBS administration. All experiments and procedures were performed in accordance with the NIH Guide for the Care and Use of Laboratory Animals and were approved by the Massachusetts General Hospital Institutional Animal Care and Use Committee.

Probes

Three gadolinium-based molecular probes were used in this study. EP-2104R and EP-3533 were purchased from Collagen Medical LLC (Belmont, MA). EP-2104R comprises an 11 amino acid peptide derivatized with four Gd-DOTA chelates and has affinity for fibrin (K_d = 1.7 μM). The relaxivity of EP-2104R at 1.4T was reported to be 40.3 in Tris buffered saline, 44.2 in fibrinogen solution and 71.4 $mM^{-1}s^{-1}$ per molecule of EP-2104R in fibrin gel (note that there are 4 Gd per peptide, so the per Gd relaxivity is 4 times lower) (21). A linear peptide control (CLP) probe was synthesized by reduction of the disulfide bond in EP-2104R followed by alkylation of the cysteine thiols with iodoacetic acid as described by Uppal et al. (25). The binding of CLP to fibrin was assessed in a direct binding assay and showed no detectable affinity.

EP-3533 comprises a ten amino acid cyclic peptide conjugated to three Gd-DTPA (27). The peptide has affinity for type I collagen (K_d = 1.8 μM) and relaxivity of 48.3 $mM^{-1}s^{-1}$ per molecule (16.1 $mM^{-1}s^{-1}$ per Gd) at 1.4T, 37 °C (27). In the liver, molecular imaging of collagen with EP-3533 has been shown to accurately stage liver fibrosis (28, 29).

Relaxivity of CLP

Relaxivity was determined at 1.4 T, 37 °C using a Bruker mq60 Minispec. Solutions of varying concentrations of CLP were prepared in Tris buffered saline, in 5 mg/mL human fibrinogen, or in 5 mg/mL fibrinogen solutions that had been converted to fibrin gels by addition of $CaCl_2$ and thrombin following the procedure previously reported (21). For the fibrinogen and fibrin samples, the concentration of CLP was always lower than that of fibrinogen or fibrin. Concentration of Gd was determined by ICP-MS and T_1 was measured using an inversion recovery sequence. Relaxivity was determined from the slope of a plot of $1/T_1$ versus concentration. The relaxivity of EP-2104R was also measured under the same conditions.

Pharmacokinetic comparison of CLP and EP-2104R

Six male Wistar rats were anesthetized with isoflurane and the left femoral artery and left femoral vein were cannulated. The femoral artery was used to deliver either CLP (n=3) or EP-2104R (n=3) as a bolus at a dose of 5 μmol/kg. Blood was then sampled from the femoral vein at 1, 3, 5, 10, 20, 40, and 60 minutes. The plasma was separated and analyzed for Gd concentration by ICP-MS. The Gd concentration versus time curves were fit to a biexponential function to estimate the distribution and elimination half-lives of each contrast agent.

Imaging and Image analysis

Imaging was performed on a human whole-body 1.5T system (Avanto, Siemens Healthcare) with a custom-built solenoid transmit-receive coil. Animals were anesthetized with isoflurane (1–2%) for the duration of the experiment. The tail vein was cannulated for intravenous delivery of contrast media. Three different imaging paradigms were used as explained below.

a) Fibrin-targeted EP-2104R in liver fibrosis in the presence and absence of inflammation—Rats dosed with DEN for four weeks were imaged one day (inflammatory phase, n=6), or seven days after the last DEN administration (n=6). Control rats were administered PBS for four weeks and imaged 7 days after the last administration (n=5). All rats were imaged prior to and immediately following intravenous bolus injection of 5 μmol/kg EP-2104R with a T1-weighted 3D gradient echo VIBE (Volumetric Interpolated Breath-hold Examination) sequence. Imaging was repeated continuously for 30 minutes following contrast delivery. Rats were euthanized at the end of the imaging session and liver tissue was subjected to histologic analysis.

b) Comparison of CLP and EP-2104R enhancement in liver fibrosis in the presence and absence of inflammation—A second group of DEN animals (1 day post DEN, n=6; 7 days post DEN, n=5) were imaged with a series of baseline 3D VIBE images followed by a bolus injection of 5 μmol/kg CLP control probe, and serial VIBE imaging for 45 minutes. Then, 5 μmol/kg of EP-2104R was given as a bolus and the imaging repeated for 30 minutes. Following imaging, animals were sacrificed and tissue was collected for histologic analysis.

c) Comparison of fibrin-targeted (EP-2104R) and collagen-targeted (EP-3533) MRI in liver fibrosis in the presence and absence of inflammation—DEN was administered to rats (n=8) for 5 weeks. One day after the last DEN administration rats were imaged with a series of baseline 3D VIBE scans and a 3D Inversion Recovery (IR) FLASH (Fast Low Angle Shot) T1 mapping sequence. EP-2104R, 5 μmol/kg, was given as an i.v. bolus and the VIBE sequence was repeated for 30 minutes post injection. Next, the T1 map was repeated followed by a 10 μmol/kg bolus of EP-3533, and then another T1 map recorded one hour after the EP-3533 injection. Following the imaging session, rats were returned to their cages for 6 days and then the same scan protocol with both probes was repeated.

Fibrin-targeted imaging: The VIBE sequence was respiratory-triggered with acquisition parameters including: echo time (TE) = 1.84 ms, field-of-view (FOV) = 120×93 mm^2, matrix = 192×150, 36 slices, slice thickness = 0.6 mm, 1 average. Repetition time (TR) was equal to the length of the respiratory cycle. Mean signal intensity (SI) of liver parenchyma was estimated at baseline (SI_{pre}) and at various time points after contrast injection (SI_{post}). Percent change in post-contrast liver SI relative to baseline was calculated as: $\%\Delta SI=100*(SI_{post} - SI_{pre})/SI_{pre}$ for all imaging time points. %ΔSI was plotted as a function of time to obtain a time-signal intensity curve. The area under this curve (AUC) for the first 15 minutes of imaging post injection was calculated.

Collagen-targeted imaging: IR FLASH was performed as previously described.(29) Briefly, images were acquired with inversion recovery times of 50, 100, 200, 250, 300, 400 and 1000 ms. Acquisition parameters included TE = 2.44 ms, FOV = 120×93 mm^2, matrix = 192×150, 36 slices, slice thickness = 0.6 mm. The effective TR was dictated by the respiration rate. Changes in longitudinal relaxation rate (ΔR1) induced by EP-3533 were calculated by fitting the inversion recovery signal intensities as a function of the inversion recovery time.

All image processing was performed in MATLAB (Mathworks, Natick, MA).

Tissue analysis

Formalin-fixed samples were embedded in paraffin, cut into 5 μm-thick sections and stained with Sirius Red for fibrosis and hematoxylin and eosin (H&E) for inflammation according to standard procedures. Immunohistochemistry was performed using monoclonal fibrin antibody (product NYBT2G1 at 1:25 dilution; Accurate Chemical and Scientific Corp, Westbury, NY) following the manufacturer's recommended protocol. The H&E and Sirius Red slides were reviewed by a board certified pathologist using a modified histological activity index (HAI) for fibrosis (0 – 6) and also for inflammation scale (0 – 4), according to the method of Ishak (30). Collagen Proportional Area (CPA) as determined by the % area stained with Sirius Red, was quantified from the histology images using ImageJ (28, 31).

Statistical Analysis

All data are reported as the mean ± standard error. Differences among groups were evaluated with either paired or unpaired Student's t-test. In all tests, a P value < 0.05 was considered to be significant.

Results

Relaxivity of EP-2104R and CLP

The relaxivities of EP-2104R and CLP measured in Tris buffered saline (TBS), in 5 mg/mL fibrinogen / TBS solution, and in 5 mg/mL fibrin gel in TBS are shown in Table 1. The relaxivities of EP-2104R and its linear peptide control, CLP, are very similar when measured in TBS or in fibrinogen solution. However in fibrin gel the relaxivity of EP-2104R is increased 82% relative to the value in fibrinogen solution while for CLP an increase of 5.5% was observed. The increased relaxivity of EP-2104R in fibrin is due to protein binding resulting in an increased rotational correlation time. Since CLP does not bind fibrin, there was no significant increase in relaxivity in fibrin gel (21).

Pharmacokinetics of EP-2104R and CLP in rats

Both EP-2104R and CLP exhibited bi-exponential plasma clearance in rats consistent with a two-compartment model where there is a distribution phase with a short half-life and an elimination phase with a longer half-life. The clearance rates were very similar as expected for compounds of similar size exhibiting an extracellular distribution. Fitting the plasma concentration versus time to a biexponential gives a distribution phase half-life for EP-2104R of 1.0 ± 0.3 min compared to 1.2 ± 0.3 min for CLP, P=0.55, and an elimination phase half-life for EP-2104R of 20.4 ± 2.1 min compared to 18.1 ± 2.1 min for CLP, P=0.32.

Diethylnitrosamine (DEN) model of hepatic fibrosis and inflammation.

Rats weighed 190 – 220 g at the beginning of the study. After 4 weekly i.p. injections of 100 mg/kg diethylnitrosamine (DEN), the rat liver becomes moderately fibrotic, and the rats weigh less than rats that received PBS injections (DEN: 301 ± 4 vs PBS: 401 ± 8 g, P<0.0001). One day after the last DEN administration, the liver is inflamed, as indicated by the H&E stained sections which show an abundance of inflammatory cells, Figure 1A, and fibrotic, as indicated by the positive Sirius Red stained liver sections, Figure 1B. Immunostaining for fibrin reveals substantial positive extravascular involvement, Figure 1C. However if the liver is analyzed 7 days after the last DEN administration, fibrosis is still present, but the inflammation has largely resolved, and there is no evidence of fibrin immunostaining. In rats administered PBS vehicle there is no evidence of fibrosis nor inflammation. Quantification of Sirius Red staining to give the collagen proportional area (CPA) showed significantly elevated CPA for the two DEN groups compared to PBS controls (PBS: 0.38 ± 0.10 % vs 1 day post DEN: 3.14 ± 1.27 %, P<0.01; PBS vs 7 days post DEN: 3.30 ± 0.65%, P<0.001), but there was no difference between the DEN animals sacrificed one day or 7 days after the last DEN administration, P=0.8, Figure 1D. Similarly the fibrosis Ishak score for the PBS controls was 0 but significantly higher for 1 day post DEN: 3.62 ± 0.31, P<0.0001, and for 7 days post DEN: 3.82 ± 0.25, P<0.0001. However

there was no significant difference (P=0.60) in Ishak score between the DEN animals sacrificed one day or 7 days after the last DEN administration. On the other hand the HAI score for inflammation was significantly different among the three groups of rats and was highest 1 day post DEN: 3.54 ± 0.14 which was significantly greater than at 7 days post DEN: 1.61 ± 0.16, P<0.0001 or the PBS controls: 0.40 ± 0.24, P<0.0001. The 7 day post DEN score was also significantly higher than the PBS controls, P<0.01. Quantification of the fibrin immunostaining showed significantly higher area stained in the 1 day post DEN: 3.56 ± 1.35 which was significantly greater than at 7 days post DEN: 1.02 ± 0.58, P<0.0001 or the PBS controls: 0.67 ± 0.26, P<0.0001.

EP-2104R provides increased liver enhancement in DEN injured rats compared to controls

To determine whether EP-2104R-enhanced MRI could detect fibrin deposition and inflammation in response to acute injury, DEN-injured rats were imaged 1 day or 7 days following the 4th dose of DEN and compared to PBS control rats. MRI signal enhancement characteristics (peak percent increase in signal intensity compared to baseline (%ΔSI) and the area under the curve (AUC) for the increase in signal intensity post probe injection over the duration of the study) following EP-2104R injection were all higher in both groups of DEN injured rats than in PBS control rats. Figure 2A shows representative axial MR images with a false color overlay of the Post – Pre image at one minute post injection. Rats imaged 7 days post DEN administration demonstrated a 32% higher change in peak liver SI compared to controls (control: 17.0 ± 0.2%, 7 day post DEN: 22.4 ± 2.0%, p = 0.017), Figure 2B, even though hepatic fibrin was not histologically detected in this cohort. By comparison, rats imaged 1 day post DEN exhibited even larger peak %ΔSI: 71% higher than controls (controls: 17.0 ± 0.2%, 1 day post DEN: 29.0 ± 3.2%, p=0.017) and 29% higher than the 7 day post DEN group (p=0.021), Figure 2B, even though these two cohorts had similar levels of fibrosis. Similar findings were observed when comparing the AUC among these groups, Figure 2C. The increased signal observed in the 1 day post DEN group may be attributed to fibrin binding which will serve to both increase relaxivity as well provide some retention in tissue.

EP-2104R enhanced MRI is fibrin-specific during the inflammatory phase of liver fibrosis

To investigate whether the stronger signal enhancement observed with EP-2104R in DEN-treated rats relative to control animals is specific to fibrin accumulation, two additional groups of animals (7 day post DEN, n=5; 1 day post DEN, n=6) were generated and imaged with both EP-2104R and a non-fibrin binding control probe termed CLP. The disulfide-bridged cyclic peptide structure of EP-2104R is necessary for fibrin binding. We used a linear peptide analog of EP-2104R, CLP, wherein the cysteine residues are modified to thioethers, and this modification results in no measurable binding to fibrin. However CLP has similar pharmacokinetics to EP-2104R. The relaxivity of CLP is very similar to EP-2104R in the absence of fibrin, but the relaxivity of EP-2104R bound to fibrin is 80% higher.

We performed intra-animal comparisons between EP-2104R and CLP by using sequential administration of the two probes in the same imaging session. We first injected CLP and imaged until this compound had cleared (45 minutes) and then injected EP-2104R and

imaged for an additional 20 minutes. For each animal, the same ROIs were used for characterizing enhancement with both injected probes.

Figure 3A displays representative MR signal kinetics curves in a 7 day post DEN rat illustrating similar washout behavior of CLP and EP-2104R. In fact, no statistically significant differences were observed between EP-2104R and CLP in terms of peak %ΔSI (Fig. 3B) and AUC (Fig. 3C). In addition, fibrin-positive staining was not histologically evident in this cohort. On the other hand, washout of CLP and EP-2104R differed dramatically in 1 day post DEN rats (Fig. 3D). This cohort exhibited 14% higher peak %ΔSI (Fig. 3E) and 45% larger AUC (Fig. 3F) with EP-2014R than with CLP. These results, coupled with the distinct fibrin-rich areas observed on histology (e.g. Fig. 1C), suggest that contrast enhancement differences during the inflammatory phase are specific to fibrin deposition which will result in binding by EP-2104R causing retention and increased relaxivity. By comparison, changes in extracellular volume and endothelial permeability, rather than deposition of extracellular fibrin, dominate signal enhancement patterns in DEN rats imaged 7 days after the last DEN administration where inflammation has resolved.

Collagen-targeted MR probe EP-3533 is insensitive to the presence of inflammation

To further investigate the specificity of EP-2104R for inflammation in the context of liver fibrosis, we next compared EP-2104R to the collagen-targeted probe EP-3533. A cohort of rats was first administered DEN weekly for five weeks to generate fibrosis. All rats underwent MRI twice: (1) during week 5, in the inflammatory phase 1 day post the 5th DEN dose and (2) seven days after the last DEN administration. Both imaging sessions included sequential injection of EP-2104R for evaluation of fibrin deposition followed by intravenous administration of the collagen-targeted contrast agent, EP-3533, for assessment of fibrosis. In the liver, molecular imaging of collagen with EP-3533 has been shown to accurately stage liver fibrosis.(28, 29) On EP-3533-enhanced images, there were no significant differences between mean ΔR1 measured 1 day or 7 days following the last DEN administration suggesting no change in fibrotic burden after one week of withdrawal from DEN as expected (Fig. 4A). By comparison, EP-2104R signal enhancement decreased from 1 day post DEN to 7 days post DEN as both mean peak %ΔSI and mean AUC declined by 20% when measured 7 days after withdrawal of DEN (Fig. 4B, C).

Discussion

Wound healing is a natural response to tissue injury that normally comprises a cascade of events including coagulation, inflammation, fibroproliferation, and re-epithelization. Exposure to persistent insult or dysregulation of the cascade can however result in excessive tissue scarring (fibrosis) and subsequent alterations of normal tissue structure and function (32). The etiology of liver fibrosis includes viral infections such as hepatitis B and C, aberrant lipid metabolism induced by obesity or alcohol, or cholestatic disease. If left untreated, fibrosis can progress to cirrhosis which is the major risk factor for life-threatening conditions such as hepatocellular carcinoma and liver failure. In nonalcoholic steatohepatitis (NASH), the presence of both inflammation and fibrosis are defining features which distinguish NASH from benign fatty liver disease.

The process of coagulation is also marked by a series of events which includes thrombin generation, platelet activation, and fibrin deposition. In addition to its primary function of maintaining homeostasis, coagulation is also known to play a role in downstream inflammatory and fibroproliferative processes of tissue repair (15–17). There is growing evidence that over-exuberant coagulation in liver injury promotes progression of liver fibrosis (15). Thrombus formation in the hepatic vasculature, frequently observed in both animal models and cirrhotic patients, is believed to be an indicator of hypercoagulation (33, 34). The pro-fibrotic role of increased coagulation activity is highlighted by slower progression of fibrosis in patients with hemophilia (35), and faster disease progression in carriers of an FV Leiden mutation, a cause of hereditary hypercoagulopathy (36). In addition, anticoagulant drugs, including heparins, vitamin K antagonists, aspirin, and the direct thrombin inhibitor dabigatran, have been shown to slow down disease progression in a variety of animal models of liver fibrosis (20, 37–40). Therapeutic effects of anticoagulants have also been reported in patients with fibrosis or cirrhosis (41, 42). The precise mechanisms linking coagulation to hepatic fibrosis remain incompletely understood and a subject of active research.

Fibrin, the end product of coagulation, is a result of thrombin-mediated conversion of fibrinogen to an insoluble fibrin network. Abnormal extravascular, parenchymal accumulation of fibrin has been previously detected in rodent models of hepatic fibrosis (18–20). Extravascular fibrin deposition is anticipated after acute injury due to vascular leakage caused by endothelial damage. In fact, elevated fibrinogen/fibrin levels were present along sinusoids and in areas of necrosis following acute injury in rats treated with carbon tetrachloride (CCl_4) (18). Histological evidence for abnormal fibrin accumulation after extended exposure to injury also exists. For example, abnormal fibrin deposits were observed in fibrous septa following repeat injury (18). In a cholestatic disease model induced with α-napthylisothiocyanate (ANIT) in mice, increased peribilliary and sinusoidal fibrin deposition was evident in ANIT-treated mice as compared to control animals (19). Fibrin was detected in liver sinusoids of mice fed high-fat diet (HFD) for 2 and 3 months to induce nonalcoholic fatty liver disease but not in animals on control diet. In addition, fibrin deposition preceded an increase in plasma thrombin-antithrombin levels. More importantly, administration of the direct thrombin inhibitor dabigatran reduced hepatic inflammation and injury in parallel with the reduction in fibrin deposition (20).

Here, we sought to determine whether molecular imaging of extravascular fibrin could be a useful way to assess hepatic inflammation. The fibrin probe EP-2104R has demonstrated efficacy in the detection of thrombus, but also in quantifying extravascular fibrin associated with cancer or pulmonary inflammation (23–26). EP-2104R has rapid plasma clearance and no hepatobiliary elimination resulting in low non-specific liver enhancement (43). The magnitude of peak %ΔSI observed with any small molecular weight contrast agent targeting the interstitial space will depend on vessel permeability, extracellular volume, target concentration, and relaxivity. Given that extracellular volume is known to increase in fibrotic tissue (44), the signal enhancement observed between healthy and DEN-injured livers imaged 7 days after the last DEN insult were likely a consequence of the larger extracellular volume in the fibrotic cohort and not specific to fibrin accumulation which was not detected by IHC. By comparison, the stronger signal in observed one day after the last DEN insult is

likely a result of both increased permeability caused by inflammation as well as increased fibrin accumulation as confirmed by histology and unique to this group. The presence of fibrin results in higher relaxivity for EP-2104R. This hypothesis was further supported by the direct comparison with the non-binding control peptide CLP which showed identical liver enhancement to EP-2104R in rats 7 days post DEN when inflammation (and fibrin) was absent but significantly lower liver enhancement than EP-2104R during the inflammatory phase 1 day post DEN when fibrin was present. These studies also demonstrate that fibrin/inflammation can be imaged on a background of liver fibrosis. On the other hand, the results with the collagen-specific probe EP-3533 indicated that this probe is sensitive only to fibrosis, in the presence or absence of inflammation.

Determination of the specific role of the coagulation cascade and fibrin deposition in the development of liver fibrosis was not the goal of this study. It is conceivable that thrombin activation and extravascular fibrin deposition are simply a byproduct of vascular leak in response to tissue injury, but there is some evidence that it is an early mediator of disease pathogenesis in the liver. Our data suggest that fibrin deposition is highly correlated with the extent of inflammation as both are detected only in the acute phase of injury and resolve within a week. For this reason, EP-2104R-enhanced MRI could serve as a biomarker for tissue injury and inflammation and may be used to monitor disease improvement in response to therapeutic intervention.

There are some limitations to this study. First, EP-2104R was evaluated in a single animal model of toxin induced fibrosis and inflammation. While dietary models may better recapitulate the steatosis, inflammation, and fibrosis that occurs in NASH, the DEN model used here allowed us to generate liver fibrosis with controlled high or low levels of inflammation, and to show that extravascular fibrin is a useful marker of hepatic inflammation. Future work should evaluate this technique in other models of liver inflammation. A second limitation was that there was no dose range finding to establish the optimal dose of EP-2104R. The dose was chosen based on prior thrombus imaging studies, but a higher dose may render inflammation more conspicuous although it may also increase non-specific enhancement.

Conclusion

EP-2104R enhanced MRI can specifically detect liver injury and fibrin associated with inflammation in the presence of liver fibrosis. Fibrin may be a useful imaging biomarker to detect liver inflammation and to monitor treatment response.

Sources of Support:

This work was supported by grants from the National Institutes of Health (DK104956, DK104302, EB009062, and OD010650).

References

1. Williams R Global challenges in liver disease. Hepatology. 2006;44(3):521–6. [PubMed: 16941687]

2. Vernon G, Baranova A, Younossi ZM. Systematic review: the epidemiology and natural history of non-alcoholic fatty liver disease and non-alcoholic steatohepatitis in adults. Aliment Pharmacol Ther. 2011;34(3):274–85. [PubMed: 21623852]

3. Marchesini G, Brizi M, Bianchi G, et al. Nonalcoholic fatty liver disease: a feature of the metabolic syndrome. Diabetes. 2001;50(8):1844–50. [PubMed: 11473047]

4. Yokoo T, Serai SD, Pirasteh A, et al. Linearity, Bias, and Precision of Hepatic Proton Density Fat Fraction Measurements by Using MR Imaging: A Meta-Analysis. Radiology. 2018;286(2):486–98. [PubMed: 28892458]

5. Caussy C, Reeder SB, Sirlin CB, Loomba R. Noninvasive, Quantitative Assessment of Liver Fat by MRI-PDFF as an Endpoint in NASH Trials. Hepatology. 2018;68(2):763–72. [PubMed: 29356032]

6. Lieber CS, Weiss DG, Paronetto F. Value of fibrosis markers for staging liver fibrosis in patients with precirrhotic alcoholic liver disease. Alcohol Clin Exp Res. 2008;32(6):1031–9. [PubMed: 18422837]

7. Parkes J, Guha IN, Roderick P, Rosenberg W. Performance of serum marker panels for liver fibrosis in chronic hepatitis C. J Hepatol. 2006;44(3):462–74. [PubMed: 16427156]

8. Park CC, Nguyen P, Hernandez C, et al. Magnetic Resonance Elastography vs Transient Elastography in Detection of Fibrosis and Noninvasive Measurement of Steatosis in Patients With Biopsy-Proven Nonalcoholic Fatty Liver Disease. Gastroenterology. 2017;152(3):598–607 e2. [PubMed: 27911262]

9. Imajo K, Kessoku T, Honda Y, et al. Magnetic Resonance Imaging More Accurately Classifies Steatosis and Fibrosis in Patients With Nonalcoholic Fatty Liver Disease Than Transient Elastography. Gastroenterology. 2016;150(3):626–37 e7. [PubMed: 26677985]

10. Farrar CT, Gale EM, Kennan R, et al. CM-101: Type I Collagen-targeted MR Imaging Probe for Detection of Liver Fibrosis. Radiology. 2018;287(2):581–9. [PubMed: 29156148]

11. Erstad DJ, Farrar CT, Ghoshal S, et al. Molecular magnetic resonance imaging accurately measures the antifibrotic effect of EDP-305, a novel farnesoid X receptor agonist. Hepatol Commun. 2018;2(7):821–35. [PubMed: 30027140]

12. Zhu B, Wei L, Rotile N, et al. Combined magnetic resonance elastography and collagen molecular magnetic resonance imaging accurately stage liver fibrosis in a rat model. Hepatology. 2017;65(3):1015–25. [PubMed: 28039886]

13. Chen HH, Waghorn PA, Wei L, et al. Molecular imaging of oxidized collagen quantifies pulmonary and hepatic fibrogenesis. JCI Insight. 2017;2(11).

14. Pulli B, Wojtkiewicz G, Iwamoto Y, et al. Molecular MR Imaging of Myeloperoxidase Distinguishes Steatosis from Steatohepatitis in Nonalcoholic Fatty Liver Disease. Radiology. 2017;284(2):390–400. [PubMed: 28358240]

15. Chambers RC, Laurent GJ. Coagulation cascade proteases and tissue fibrosis. Biochem Soc Trans. 2002;30(2):194–200. [PubMed: 12023850]

16. Mercer PF, Chambers RC. Coagulation and coagulation signalling in fibrosis. Biochim Biophys Acta. 2013;1832(7):1018–27. [PubMed: 23298546]

17. Platelets Lisman T. and fibrin in progression of liver disease: friends or foes? J Thromb Haemost. 2015;13(1):54–6. [PubMed: 25393399]

18. Neubauer K, Knittel T, Armbrust T, Ramadori G. Accumulation and cellular localization of fibrinogen/fibrin during short-term and long-term rat liver injury. Gastroenterology. 1995;108(4):1124–35. [PubMed: 7698580]

19. Joshi N, Kopec AK, O'Brien KM, et al. Coagulation-driven platelet activation reduces cholestatic liver injury and fibrosis in mice. J Thromb Haemost. 2015;13(1):57–71. [PubMed: 25353084]

20. Kopec AK, Joshi N, Towery KL, et al. Thrombin inhibition with dabigatran protects against high-fat diet-induced fatty liver disease in mice. J Pharmacol Exp Ther. 2014;351(2):288–97. [PubMed: 25138021]

21. Overoye-Chan K, Koerner S, Looby RJ, et al. EP-2104R: a fibrin-specific gadolinium-Based MRI contrast agent for detection of thrombus. J Am Chem Soc. 2008;130(18):6025–39. [PubMed: 18393503]

22. Stracke CP, Katoh M, Wiethoff AJ, et al. Molecular MRI of cerebral venous sinus thrombosis using a new fibrin-specific MR contrast agent. Stroke. 2007;38(5):1476–81. [PubMed: 17379818]

23. Vymazal J, Spuentrup E, Cardenas-Molina G, et al. Thrombus imaging with fibrin-specific gadolinium-based MR contrast agent EP-2104R: results of a phase II clinical study of feasibility. Invest Radiol. 2009;44(11):697–704. [PubMed: 19809344]
24. Shea BS, Probst CK, Brazee PL, et al. Uncoupling of the profibrotic and hemostatic effects of thrombin in lung fibrosis. JCI Insight. 2017;2(9).
25. Uppal R, Medarova Z, Farrar CT, et al. Molecular imaging of fibrin in a breast cancer xenograft mouse model. Invest Radiol. 2012;47(10):553–8. [PubMed: 22960948]
26. Morelli JN, Runge VM, Williams JM, et al. Evaluation of a fibrin-binding gadolinium chelate peptide tetramer in a brain glioma model. Invest Radiol. 2011;46(3):169–77. [PubMed: 21150792]
27. Caravan P, Das B, Dumas S, et al. Collagen-targeted MRI contrast agent for molecular imaging of fibrosis. Angew Chem Int Ed Engl. 2007;46(43):8171–3. [PubMed: 17893943]
28. Fuchs BC, Wang H, Yang Y, et al. Molecular MRI of collagen to diagnose and stage liver fibrosis. J Hepatol. 2013;59(5):992–8. [PubMed: 23838178]
29. Farrar CT, DePeralta DK, Day H, et al. 3D molecular MR imaging of liver fibrosis and response to rapamycin therapy in a bile duct ligation rat model. J Hepatol. 2015;63(3):689–96. [PubMed: 26022693]
30. Ishak K, Baptista A, Bianchi L, et al. Histological grading and staging of chronic hepatitis. J Hepatol. 1995;22(6):696–9. [PubMed: 7560864]
31. Polasek M, Fuchs BC, Uppal R, et al. Molecular MR imaging of liver fibrosis: a feasibility study using rat and mouse models. J Hepatol. 2012;57(3):549–55. [PubMed: 22634342]
32. Hernandez-Gea V, Friedman SL. Pathogenesis of liver fibrosis. Annu Rev Pathol. 2011;6:425–56. [PubMed: 21073339]
33. Kuroe K, Kurokawa T, Nishikimi M, et al. Effects of thromboxane A2 synthetase inhibitor on postischemic liver injury in rats. Eur Surg Res. 1991;23(1):20–6. [PubMed: 1879452]
34. Wanless IR, Wong F, Blendis LM, et al. Hepatic and portal vein thrombosis in cirrhosis: possible role in development of parenchymal extinction and portal hypertension. Hepatology. 1995;21(5):1238–47. [PubMed: 7737629]
35. Assy N, Pettigrew N, Lee SS, et al. Are chronic hepatitis C viral infections more benign in patients with hemophilia? Am J Gastroenterol. 2007;102(8):1672–6. [PubMed: 17433021]
36. Wright M, Goldin R, Hellier S, et al. Factor V Leiden polymorphism and the rate of fibrosis development in chronic hepatitis C virus infection. Gut. 2003;52(8):1206–10. [PubMed: 12865283]
37. Assy N, Hussein O, Khalil A, et al. The beneficial effect of aspirin and enoxaparin on fibrosis progression and regenerative activity in a rat model of cirrhosis. Dig Dis Sci. 2007;52(5):1187–93. [PubMed: 17372820]
38. Abe W, Ikejima K, Lang T, et al. Low molecular weight heparin prevents hepatic fibrogenesis caused by carbon tetrachloride in the rat. J Hepatol. 2007;46(2):286–94. [PubMed: 17166617]
39. Anstee QM, Goldin RD, Wright M, et al. Coagulation status modulates murine hepatic fibrogenesis: implications for the development of novel therapies. J Thromb Haemost. 2008;6(8):1336–43. [PubMed: 18485088]
40. Kassel KM, Sullivan BP, Cui W, et al. Therapeutic administration of the direct thrombin inhibitor argatroban reduces hepatic inflammation in mice with established fatty liver disease. Am J Pathol. 2012;181(4):1287–95. [PubMed: 22841818]
41. Shi J, Hao JH, Ren WH, Zhu JR. Effects of heparin on liver fibrosis in patients with chronic hepatitis B. World J Gastroenterol. 2003;9(7):1611–4. [PubMed: 12854176]
42. Villa E, Camma C, Marietta M, et al. Enoxaparin prevents portal vein thrombosis and liver decompensation in patients with advanced cirrhosis. Gastroenterology. 2012;143(5):1253–60 e1–4.
43. Uppal R, Catana C, Ay I, et al. Bimodal thrombus imaging: simultaneous PET/MR imaging with a fibrin-targeted dual PET/MR probe--feasibility study in rat model. Radiology. 2011;258(3):812–20. [PubMed: 21177389]
44. Wanless IR CJ. Cirrhosis. In: Odze RDGJ, Crawford JM, ed. Surgical pathology of the GI tract, liver, biliary tract, and pancreas. Philadelphia, Pa: Elsevier; 2004.

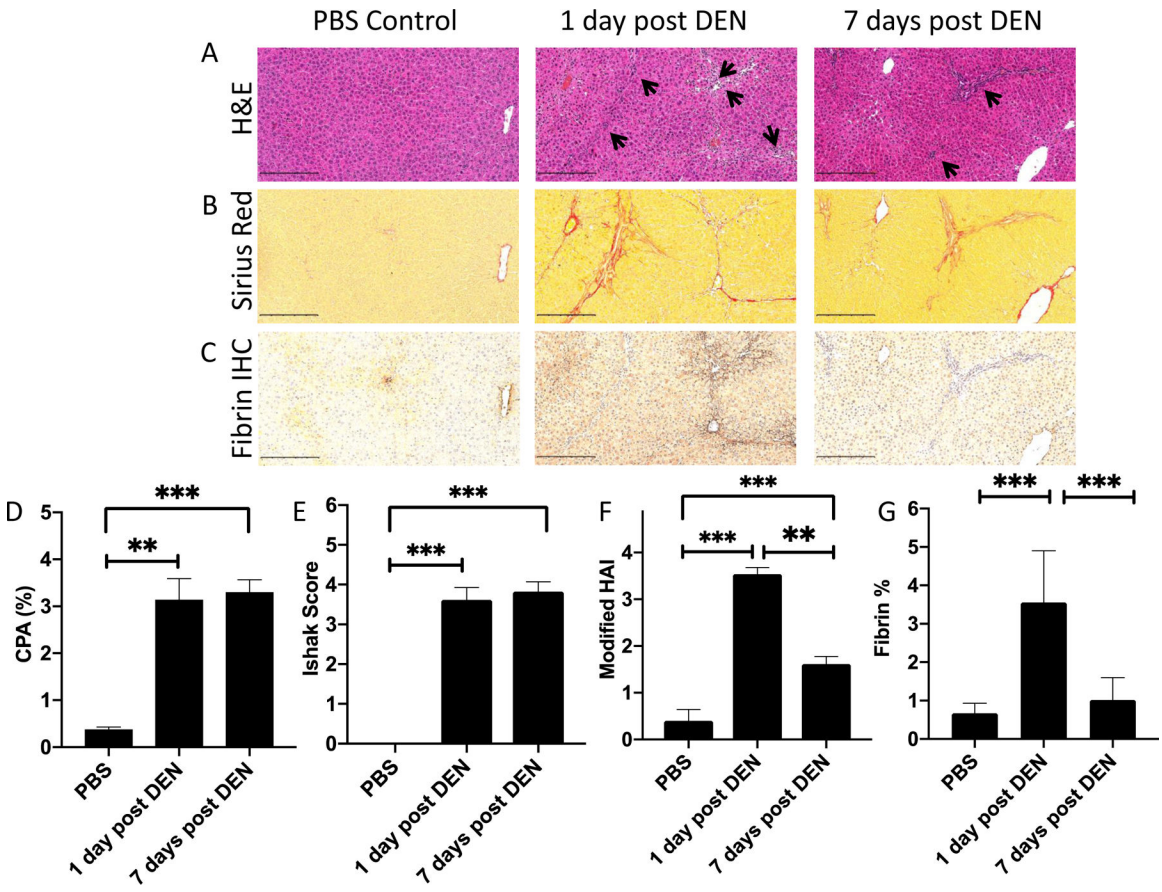

Figure 1.

Histological analysis of liver specimens from rats given 4 weekly i.p. doses of PBS (left) or 100 mg/kg of DEN and sacrificed at 1 day (middle) or 7 days (right) following the last DEN administration, scale bar = 250 μm. (A) Hematoxylin and eosin (H&E) staining of liver tissue. Inflammatory regions are labeled with pointed black arrows. (B) Sirius Red staining of liver tissue. Fibrosis is shown by intense red staining of collagen fibers. (C) Immunohistochemistry staining of fibrin in liver tissue. (D) Morphometric analysis of Sirius Red stained slides to give collagen proportional area showing moderate fibrosis in both DEN groups that is significantly higher than in PBS controls. (E) Ishak scoring of liver fibrosis showing moderate fibrosis in both DEN groups that is significantly higher than in PBS controls. (F) Histological activity index for inflammation (0 – 4) showing that inflammation is significantly higher at 1 day post DEN than 7 days post DEN. (G) Morphometric analysis of the area of the slide stained positive for fibrin by immunohistochemistry. ** $P<0.01$, *** $P<0.0001$, one way ANOVA with post hoc Tukey test.

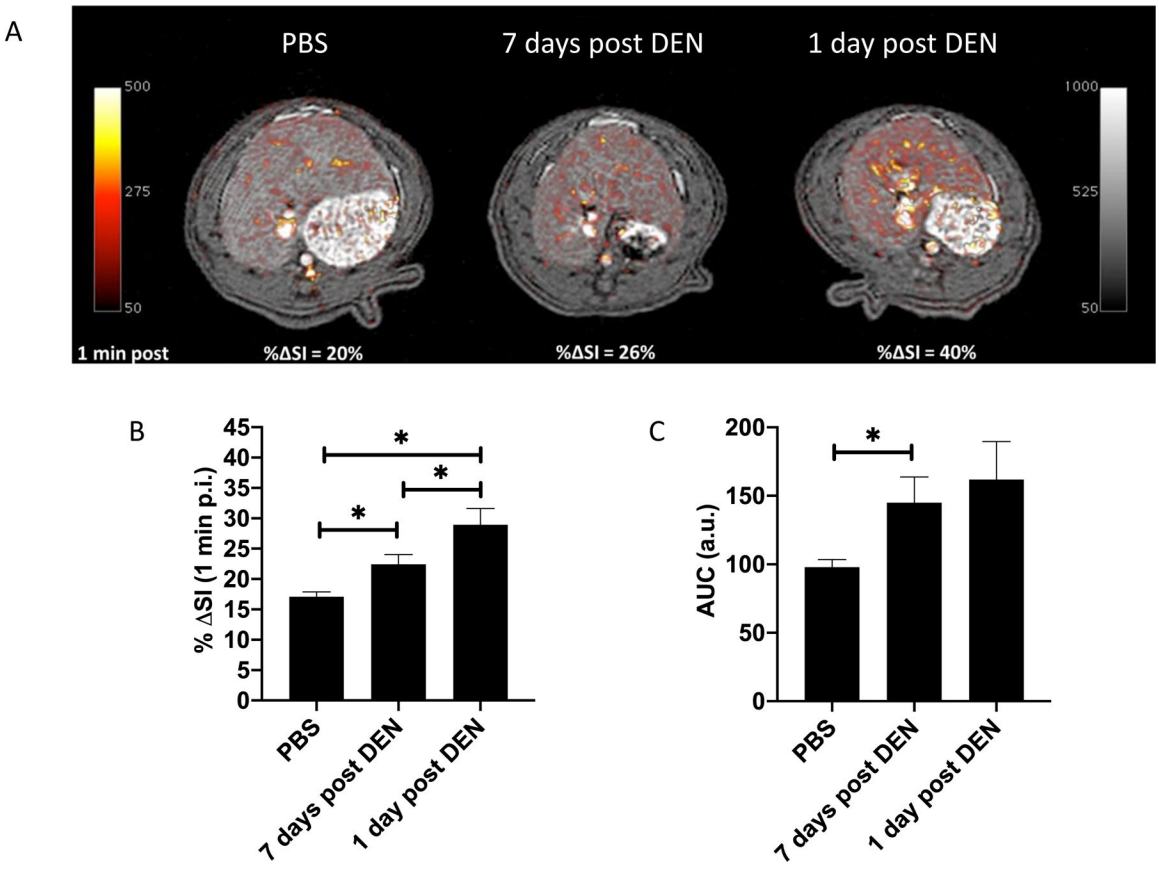

Figure 2.

(A) Representative T1-weighted axial images of rats dosed with PBS (left), with DEN and imaged 7 days after 4th DEN dose (middle), and imaged one day after 4th DEN dose (right). False color overlay represents subtraction image of pre-contrast image from the one minute post EP-2104R image. Peak liver signal enhancement (%ΔSI) at 1 min post injection of EP-2104R (B) and liver signal enhancement area under the curve (C) are significantly higher in the DEN treated rats than in PBS controls. * P<0.05, one way ANOVA with post hoc Tukey test.

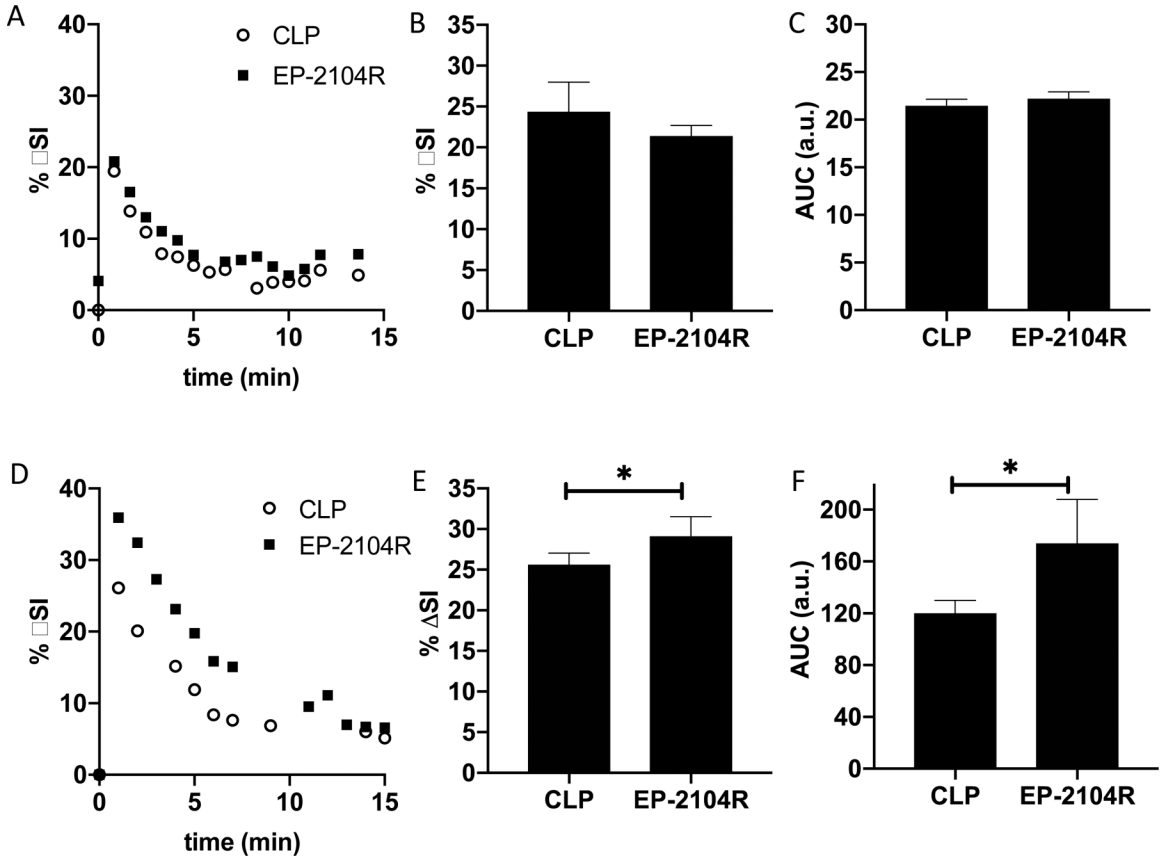

Figure 3.

Representative liver signal enhancement versus time post probe injection for EP-2014R (filled squares) and CLP (open circles) in rats imaged 7 days (A) or 1 day (D) post the last DEN dose. Peak (at 1 minute post injection) liver %ΔSI (B) and liver AUC (C) are not significantly different for EP-2104R and control probe CLP at 7 days post DEN. At 1 day post DEN, both peak liver (at 1 minute post injection) %ΔSI (E) and liver AUC (F) are significantly higher for EP-2104R indicating elevated fibrin levels during the inflammatory phase which results in increased relaxivity of EP-2104R and increased retention in liver tissue. * $P<0.05$, two tailed t-test.

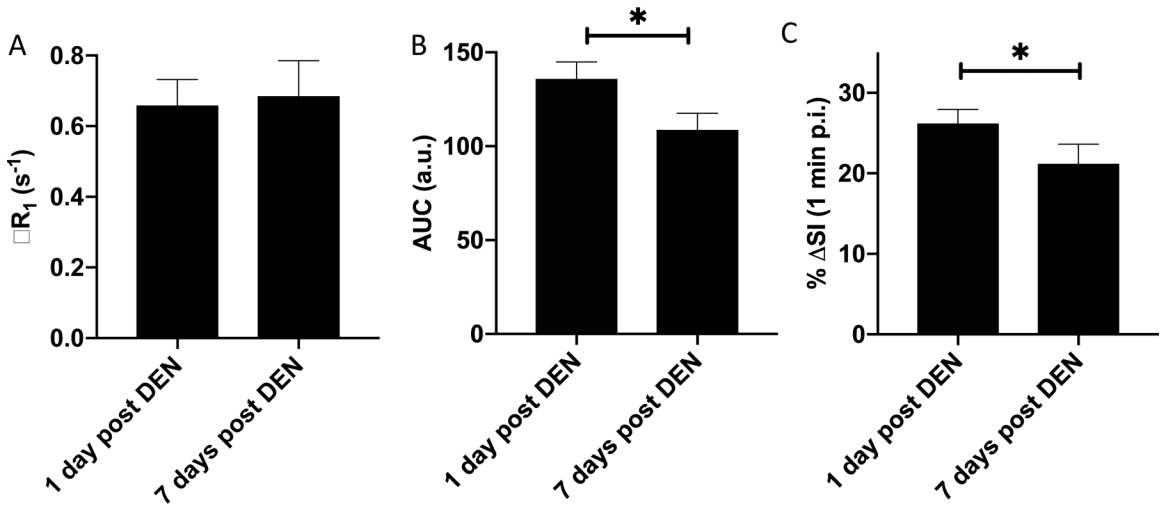

Figure 4.

(A) ΔR1 of liver after administration of collagen-targeted EP-3533 measured 1 day or 7 days following the last DEN administration. EP-3533 reports on fibrosis and this data suggests no change in fibrotic burden after one week of withdrawal from DEN as expected. Peak EP-2104R liver signal enhancement (B) and EP-2104R liver signal enhancement AUC (C) are significantly decreased from 1 day post DEN to 7 days post DEN in these animals. * $P<0.05$, two tailed t-test.

Table 1.

Relaxivity ($mM^{-1}s^{-1}$) of EP-2104R and CLP measured at 1.4 T, 37 °C in pH 7.4 50 mM Tris buffered saline (TBS), in 5 mg/mL fibrinogen / TBS solution, or in 5 mg/mL fibrin gel in TBS. Relaxivities are reported per molecule. Each probe has 4 Gd per molecule and per Gd relaxivity is the reported value divided by 4. Uncertainty in relaxivity is ± 6% based on repeated measurements in our lab.

	TBS	Fibrinogen solution	Fibrin gel
EP-2104R	39.4	39.2	71.4
CLP	38.5	41.9	44.2